Acta Cryst. (1982). A**38**, 827–835

Small-Angle Scattering: Direct Structure Analysis

BY D. I. SVERGUN AND L. A. FEIGIN

Institute of Crystallography, Academy of Sciences of the USSR, Leninsky prospekt 59, Moscow 117333, USSR

AND B. M. SCHEDRIN

Scientific Research Computer Center, Moscow State University, Moscow 117234, USSR

(*Received* 1 *March* 1982; *accepted* 21 *June* 1982)

Abstract

A direct method for structural interpretation of small-angle scattering data by monodisperse isotropic systems is presented. The spherical harmonics technique proposed by Stuhrmann [*Acta Cryst.* (1970), A**26**, 297–306] is used to choose the class of possible solutions. The method enables one to decompose scattering intensity into partial amplitudes corresponding to different multipole components of scattering density using the space and value density restrictions. If a particle possesses a rotational symmetry, its structure may be restored directly using the method; if not, additional information is required to get a set of possible solutions. The method is stable with respect to experimental errors. The efficiency of the procedure is shown in model examples. The application of the method to interpret the small-angle X-ray scattering curve of bacteriophage T7 produced a map of electron density with a resolution of about 12 Å.

Introduction

Small-angle scattering is a method widely used for the investigation of disperse isotropic systems. There are many objects – both non-organic and biological – studied by this method. Small-angle scattering data are the richest in structural information in the case when the sample is composed of a large number of independently scattering identical particles (for example dilute solutions of biological macromolecules). Under this condition the scattering intensity curve $I(s)$ [$s = (4\pi \sin \psi)/\lambda$, λ = wavelength, 2ψ = scattering angle], obtained after data processing, is proportional to the scattering intensity of a particle averaged with respect to all orientations (Guinier & Fournet, 1955). It enables one in principle to study both the shape and the internal structure of the particles.

The spherical average, however, gives rise to a considerable loss of information involved with the diffraction data, and complicates the interpretation of small-angle scattering curves. As a rule, only common geometrical and weight parameters of a particle (radius of gyration, volume, molecular weight, *etc.*) are specified directly from small-angle scattering data. Then the 'trial-and-error' method is used to estimate the structure of a particle (commonly in terms of simple geometrical bodies) in the framework of these parameters and with the aid of additional (biochemical, electron microscopy, *etc.*) information. Though the current experimental technique and processing methods permit reliable intensity curves to be obtained for a wide range of angles, a considerable share of information involved remains unutilized. Basic curves obtained by the contrast variation technique (Stuhrmann & Kirste, 1965), as well as the methods using real-space information (Glatter, 1979, 1981), except for very few special cases, fail to provide direct structure information. So one of the most important problems in the field of small-angle scattering by the systems of identical particles is the creation of a direct method aimed at the restoration of their structure, *i.e.* obtaining the scattering density distribution $\rho(\mathbf{r})$.

It is clear that the problem of obtaining a three-dimensional function $\rho(\mathbf{r})$ from a one-dimensional function $I(s)$ has an infinite variety of solutions. And, hence, the essence of any direct method should lie in a maximal possible narrowing of the class of sought solutions, physically justified restrictions being used. The direct method using the restrictions of the possible symmetry of a particle as well as its dimensions and range of density is proposed below.

Theory

For choosing the class of possible solutions it is convenient to use the approach proposed by Stuhrmann (1970). If the density $\rho(\mathbf{r})$ is supposed to be a series

$$\rho(\mathbf{r}) = \sum_{l=0}^{\infty} \sum_{m=-l}^{l} \rho_{lm}(r)\, Y_{lm}(\theta,\varphi) = \sum_{l=0}^{\infty} \rho_l(\mathbf{r}), \qquad (1)$$

0567-7394/82/060827-09$01.00

where r,θ,φ are spherical coordinates, $Y_{lm}(\theta,\varphi)$ are spherical harmonics, $\rho_{lm}(r)$ are radial functions, and

$$\rho_l(\mathbf{r}) = \sum_{m=-l}^{l} \rho_{lm}(r)\, Y_{lm}(\theta,\varphi) \qquad (2)$$

are partial multipole densities, then the intensity of small-angle scattering is

$$I(s) = 2\pi^2 \sum_{l=0}^{\infty} \sum_{m=-l}^{l} |A_{lm}(s)|^2, \qquad (3)$$

functions $\rho_{lm}(r)$ and $A_{lm}(s)$ being connected by a Hankel transform of order l:

$$A_{lm}(s) = i^l (2/\pi)^{1/2} \int_0^{\infty} \rho_{lm}(r)\, j_l(sr)\, r^2\, dr, \qquad (4)$$

$$\rho_{lm}(r) = (-i)^l (2/\pi)^{1/2} \int_0^{\infty} A_{lm}(s)\, j_l(sr)\, s^2\, ds, \qquad (5)$$

where $j_l(sr)$ are spherical Bessel functions (see *Handbook of Mathematical Functions*, 1964). Stuhrmann (1970) showed that $I(s)$ is conserved under independent rotation of any partial density $\rho_l(\mathbf{r})$. So the manifold distributions $\rho(\mathbf{r})$ determined by the same functions $\rho_{lm}(r)$ correspond to the decomposition (3), and the set of functions $\rho_{lm}(r)$ can be regarded as the variety of possible solutions introduced above.

It is clear that one can decompose intensity $I(s)$ into a sum of squares of partial amplitudes $A_{lm}(s)$, generally speaking, in an arbitrary way. To obtain the sum (3) corresponding to the true structure of a particle [*i.e.* true functions $\rho_{lm}(r)$] it is necessary to impose the restrictions on the functions $A_{lm}(s)$ according to *a priori* information on a particle. Few attempts to achieve such decomposition have been undertaken (Stuhrmann & Fuess, 1976; Marguerie & Stuhrmann, 1976); however, no general algorithm has yet been proposed.

Decomposition of the intensity into partial amplitudes

Let us suppose function $\rho(\mathbf{r})$ is adequately represented by a finite small enough number $L + 1$ of harmonics. One should bear in mind, as seen from (4), functions $A_{lm}(s)$ are independent of the value of m when functions $\rho_{lm}(r)$ are fixed. This fact means that the contributions of harmonics with different m and the same l are principally indistinguishable in the scattering intensity $I(s)$. So (3) can be rewritten as follows:

$$I(s) = 2\pi^2 \sum_{l=0}^{L} |A_l(s)|^2, \qquad (6)$$

where

$$|A_l(s)|^2 = \sum_{m=-l}^{l} |A_{lm}(s)|^2.$$

So the task is reduced to the decomposition of the scattering intensity into summands corresponding to the partial densities (2). Each term of the sum (6) determines according to (5) a radial function $\rho_l(r)$. In the case of an axially symmetric particle [$\rho_{lm}(r) \equiv 0$ if $m \neq 0$] the sum over m vanishes and we have simply $\rho_l(r) = \rho_{l0}(r)$. In the general case decomposition (6) holds, but functions $\rho_l(r)$ have no explicit physical meaning, being the superpositions of functions $\rho_{lm}(r)$.

Whatever the radial functions $\rho_{lm}(r)$ are, there are strictly specified angular non-uniformities (depending on the number of harmonic l) inherent to any partial density (2) and, therefore, there are definite regions in reciprocal space where the scattering intensity of this density $|A_l(s)|^2$ contributes maximally to $I(s)$ [in accordance with the order of the Hankel transform (4)]. Besides, the possible mode of $A_l(s)$ is also restricted by the fact that any particle is finite in space, *i.e.* such a value R exists that $\rho(\mathbf{r}) \equiv 0$ [and, therefore, $\rho_{lm}(r) \equiv 0$] if $r > R$. Fig. 1 represents the scattering amplitudes of partial densities with radial functions

$$\rho_{l0}(r) = \prod (r - R) = \begin{cases} 1, & r \leq R \\ 0, & r > R \end{cases} \qquad (7)$$

and the relative contributions of different harmonics reveal themselves well enough. Behavioral features of functions $A_l(s)$ examined above can be regarded as the physical foundation for developing an algorithm to decompose the scattering intensity into functions (6).

Indeed, suppose $L + 1$ functions $\rho_l^{(k)}(r)$, satisfying the space restrictions and determining functions $A_l^{(k)}(s)$, and, according to (6), the intensity $I^{(k)}(s)$, generally speaking, failing to coincide with $I(s)$, be specified. In order to fit the intensity $I(s)$, relative contributions of different harmonics remaining the same, one can redistribute amplitudes as follows:

$$\tilde{A}_l^{(k)}(s) = A_l^{(k)}(s)\, [I(s)/I^{(k)}(s)]^{1/2}. \qquad (8)$$

The obtained amplitudes $\tilde{A}_l^{(k)}(s)$ will obey (6), but the set $\tilde{\rho}_l^{(k)}(r)$, specified by $\tilde{A}_l^{(k)}(s)$, will not, generally speaking, meet the space restrictions. Let us, therefore, assume

$$\rho_l^{(k+1)}(r) = \tilde{\rho}_l^{(k)}(r) \prod (r - R). \qquad (9)$$

The amplitudes of the next approximation $A_l^{(k+1)}(s)$ are determined by (9) according to (4).

Thus, at each step of the iterative process determined by (8) and (9), partial amplitudes are redistributed in accordance with the number of harmonic l, value R and scattering intensity $I(s)$. Since no *a priori* information about radial functions, except space limitations, is available, step functions (7) seem to be convenient for the initial approximation.

It is possible to show the convergence of the procedure (8)–(9) to the true intensity $I(s)$ (see

Appendix *A*). To estimate the deviations in reciprocal space we have chosen the *R* factor

$$R_I = \frac{\int_0^\infty s^4[I(s) - I^{(k)}(s)]^2\,ds}{\int_0^\infty s^4 I^2(s)\,ds}. \qquad (10)$$

Since the weighting function in the metrics of reciprocal space for scattering amplitudes is a function of s^2 [see the Parseval theorem for a Hankel transform (Sneddon, 1951)] it is appropriate to introduce a factor s^4. The convergence of the process over the R_I factor is uniform.

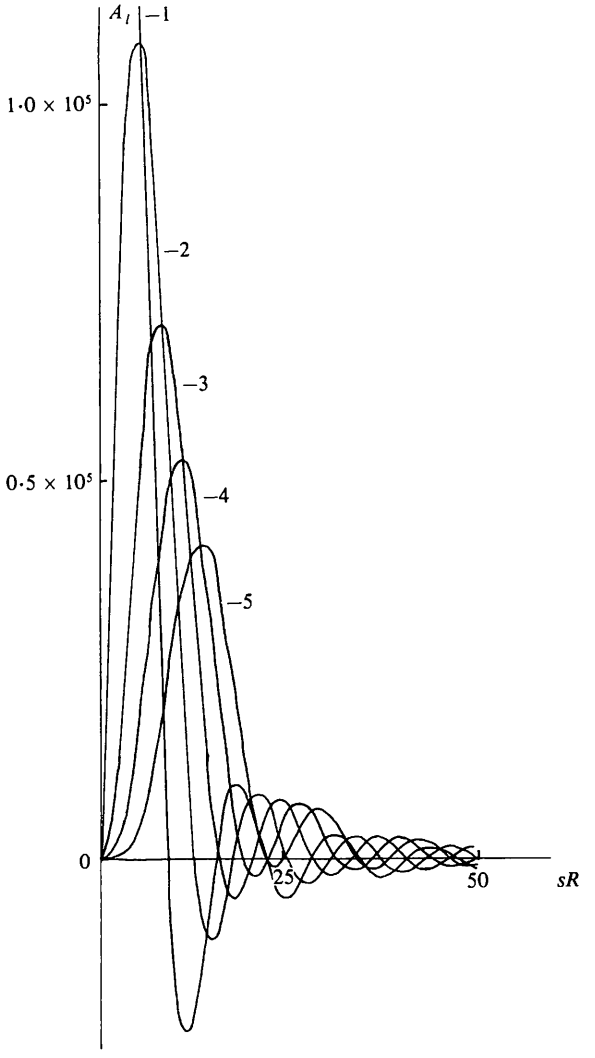

Fig. 1. Scattering amplitudes of partial densities determined by radial functions $\rho_{l0}(r) = \prod(r - R)$. Curves (1)–(5) correspond to $l = 0, 1, 2, 3, 4$; $R = 100$.

Examples

We have verified the efficiency of the procedure by means of model examples. Radial functions were specified, the intensity was calculated from them and the radial functions were restored from the intensity with procedure (8)–(9). The transformations (4)–(5) were done by the Simpson rule; termination effects in (5) (the intensities were calculated up to some finite value s_{max}) were reduced by a generalized Steklov filter (Rolbin, Svergun, Feigin & Schedrin, 1980), see Appendix *B*.

In the simplest case $L = 0$ (spherically symmetric particle) and the problem is reduced to the determination of a true set of the signs of the function $[I(s)]^{1/2}$. When the signs no longer change, the process is interrupted. Five–six iterations are enough to obtain the solution – the function $\rho_{00}(r)$ describing the structure is restored practically completely (within the range of remaining termination effects). Fig. 2 demonstrates an example of a quite unfavorable case for restoring the multistep function $\rho_{00}(r)$. The peculiarities of the application of the method for spherically symmetric particles are described in detail by Svergu ·, Feigin & Schedrin (1982).

However, when dealing with several terms of the series (6), the convergence of the process to the true intensity $I(s)$ does not guarantee the convergence to true radial functions automatically. The incorrectness of the problem (one should restore the summands from the sum of their squares) can lead to considerable distortions in the functions $\rho_l(r)$. The example of using the procedure for restoring the three model radial

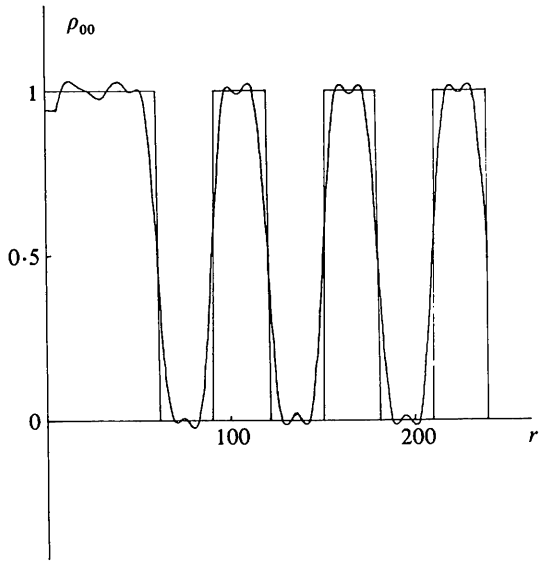

Fig. 2. The restoration of multistep spherically symmetric density distribution. Straight lines: true distribution. Solid curve: restored distribution; $R = 240$, $s_{max} = 0{\cdot}5$.

functions from their total intensity is shown in Fig. 3. The first three non-zero radial coefficients of the prolate ellipsoid of rotation with density $\rho(\mathbf{r}) = 1$, half-axes $a = 50$, $c = 100$ were chosen as model functions. The structure determined by these radial functions is reflected in Fig. 4(*a*). As is evident from Fig. 3 (curves 2) the radial functions are distorted drastically, whereas the reduction of R_I factor (Fig. 5) after some level is not involved with an appropriate improvement of the behavior of the radial functions. This is because the functions $\tilde{A}_l^{(k)}(s)$ may contain gaps leading to numerical instability of transformation (5) (especially at small r), which increases with l. Thus, it appears to be necessary to impose additional restrictions upon functions $\rho_l^{(k)}(r)$.

Density restrictions

It is natural to use the existence of the finite range of density values

$$\rho_{\min} \le \rho^{(k)}(\mathbf{r}) \le \rho_{\max} \qquad (11)$$

for $0 \le r \le R$, $0 \le \theta \le \pi$. Here

$$\rho^{(k)}(\mathbf{r}) = \sum_{l=0}^{L} \rho_l^{(k)}(r)\, Y_{l0}(\theta).$$

Indeed, the distortions in radial functions leading to considerable density fluctuations mean that conditions (11) would not be satisfied. To meet them it is necessary to introduce corrections to radial functions, the R_I factor being minimal simultaneously. Representing the corrections as a superposition of Laguerre polynomials and regarding them as small enough compared to $\rho_l(r)$, one can solve the problem by means of the linear programming technique (see Appendix *C*).

The results of including the restrictions (11) into iterative procedure (8)–(9) are seen in Fig. 3 (curves 3). It is evident that the solution with density restrictions is essentially more suitable. The R_I factor (Fig. 5) is reduced to 10^{-3}, comparable with the termination effects in (5). The restored structure composed by the radial functions obtained is given in Fig. 4(*b*). It corresponds to the initial one quite satisfactorily.

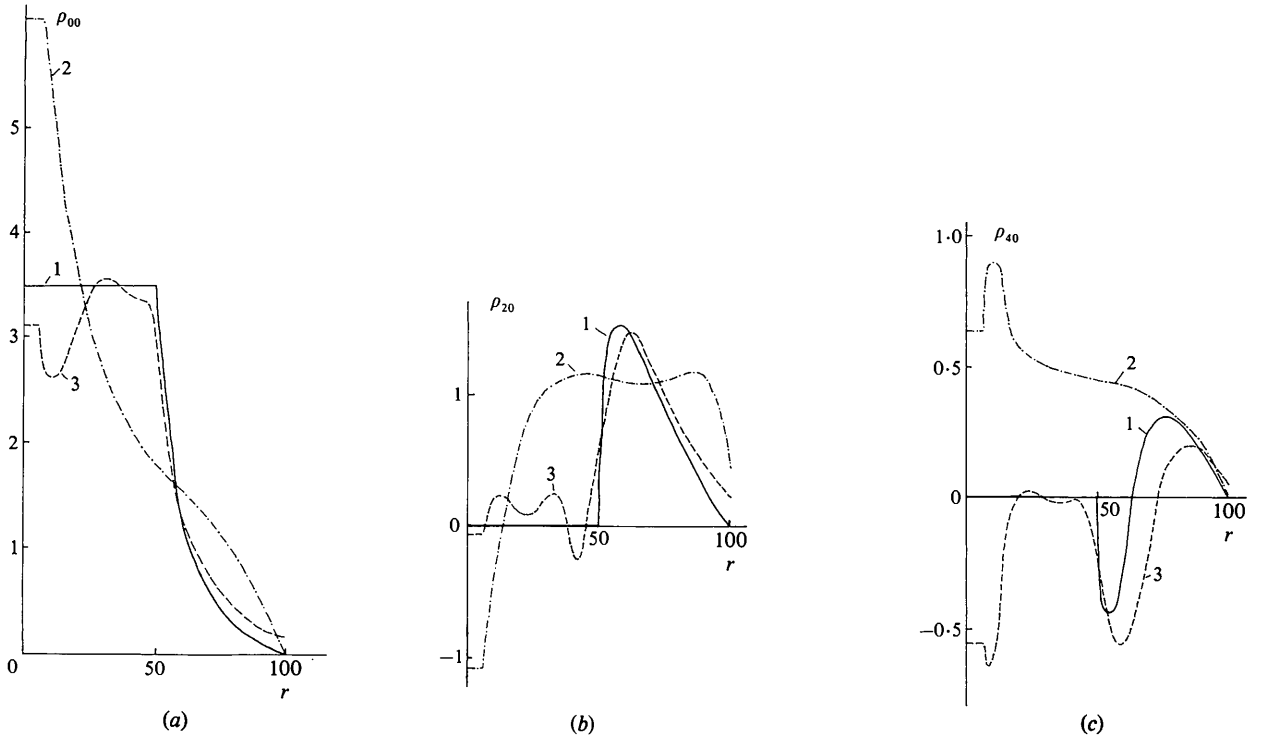

Fig. 3. The restoration of three model radial functions from the total intensity. (*a*), (*b*), (*c*) correspond to $l = 0, 2, 4$. (1) True functions $\rho_{l0}(r)$; (2) the result of the ninth iteration, $R_I = 1{\cdot}12 \times 10^{-2}$; $R = 100$, $s_{\max} = 0{\cdot}5$; (3) the result of the ninth iteration using, at fifth and eighth iterations, restrictions (11) while $\rho_{\min} = -0{\cdot}2$, $\rho_{\max} = 1{\cdot}5$; $R_I = 7{\cdot}8 \times 10^{-4}$.

The stability of the procedure

The examples given above illustrate the efficiency of the procedure with values of R, ρ_{min}, ρ_{max}, the set of harmonics as well as the function $I(s)$, exactly defined. In practice these data can be obtained with some errors, so the influence of input-data deviations on the results should be examined.

To explore the stability of the procedure with respect to the variations of the parameters R, ρ_{min}, and ρ_{max}, we used the model structure designed from the two radial coefficients of the previous example. The parameters were changed independently. Figs. 6 and 7 show the influence of the errors in R and ρ_{min}, ρ_{max} respectively. One can see that the method has good stability.

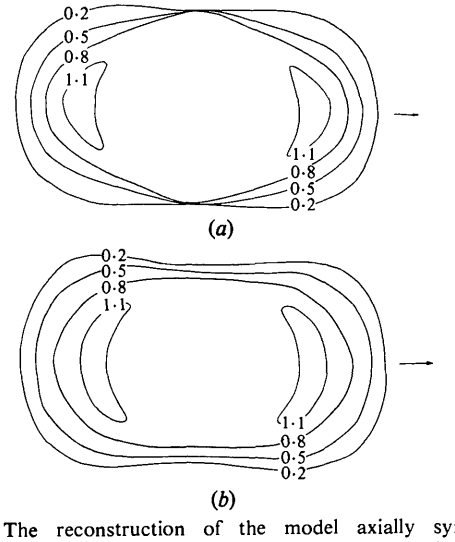

Fig. 4. The reconstruction of the model axially symmetric structure: (*a*) initial structure; (*b*) restored structure. The isolines in the cross section containing the rotation axis (indicated by an arrow) are shown.

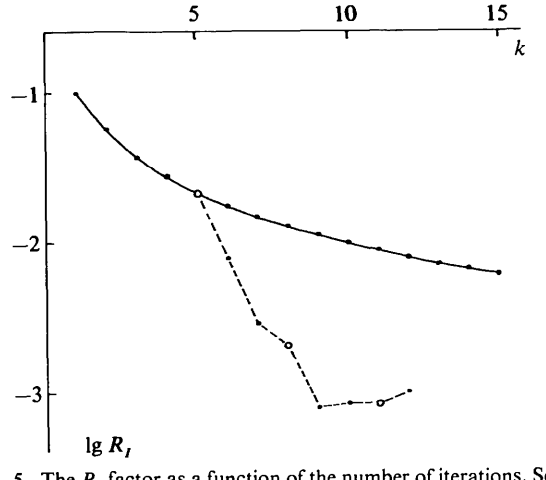

Fig. 5. The R_I factor as a function of the number of iterations. Solid curve: R_I factor of iterative process (8)–(9). Dashed line: R_I factor using restrictions (11); the iterations where restrictions have been applied are marked by circles.

In practice the errors in the set of harmonics may be connected mainly with the fact that any particle is represented, generally speaking, by an infinite series (1), whereas we are searching for a finite representation (6). Fortunately, in the case of globular particles, the first few terms of the series over spherical harmonics would describe the entire structure with sufficient precision. Fig. 8 represents the restoration from its intensity curve of the model body made up of two touching solid spheres. The reconstruction seems to be well enough (in the framework of the radial resolution determined by the value s_{max}).

The question about the set of harmonics included in the scattering intensity is closely linked with the problem of restoring the structure in the general case. If a particle possesses no axial symmetry, the iterative procedure is applicable when one can for each l specify an m' such that the function $A_{lm'}(s)$ will make the major contribution to the scattering intensity of density (2),

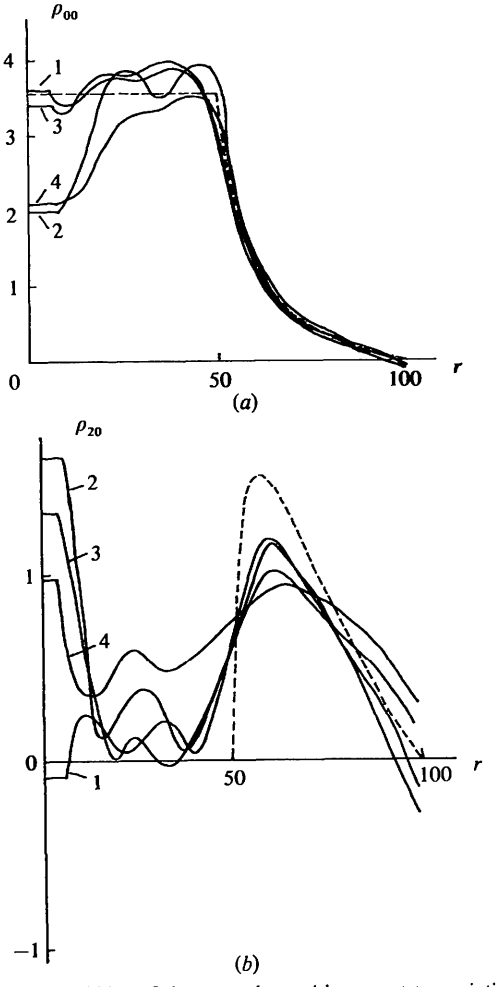

Fig. 6. The stability of the procedure with respect to variations in R. (*a*), (*b*) correspond to $l = 0, 2$. Curves (1)–(4) correspond to $R = 90, 95, 105, 110$. Dashed lines: true radial functions.

and, therefore, assign each function $\rho_l(r)$ to a definite harmonic $Y_{lm'}(\theta,\varphi)$. This, if possible, requires additional information about the particle. Choosing one (or several) relevant structures one should analyze independent rotations of densities (2) (the problem is much easier in the axially symmetric case since any rotation of partial density at an angle not equal to π, distorts the rotational symmetry).

The errors in the experimental function $I(s)$ may also lead to distortions of functions $\rho_l(r)$. It should be noted, however, that, radial functions being connected with partial amplitudes by integral transformations, small systematic errors in $I(s)$ resulting from data processing (the reduction of statistical noise, desmearing) cannot introduce considerable distortions in $\rho_l(r)$. The termination of the experimental data was taken into account by using the finite range $0 < s \leq s_{max}$ in reciprocal space. This fact has influenced mainly the radial resolution of the restored radial functions $\rho_l(r)$.

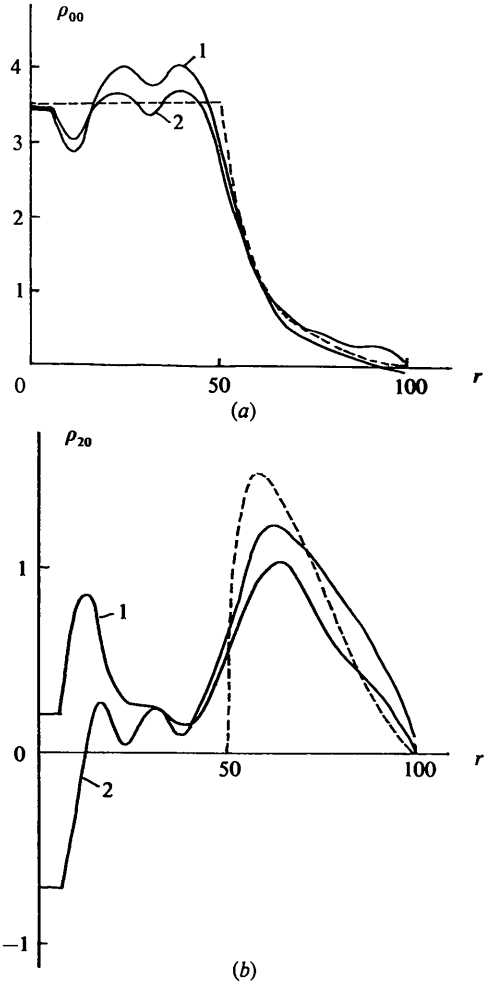

Fig. 7. The stability of the procedure with respect to variations in limiting density values. The notation is as in Fig. 6. Curve (1) corresponds to $\rho_{min} = -0{\cdot}3$, $\rho_{max} = 1{\cdot}7$; curve (2) to $\rho_{min} = 0$, $\rho_{max} = 1{\cdot}3$. True limiting values are $\rho_{min} = -0{\cdot}15$, $\rho_{max} = 1{\cdot}5$.

The practical example

As an example of a practical application of the method to a concrete structure investigation we shall adduce some results obtained from the small-angle scattering curve of bacteriophage T7. This large bacterial virus has been recently studied by different physical and other methods and possesses an approximately axially symmetric constitution – isometrical polyhedrical head and cylindrical tail, see Rolbin, Svergun, Feigin, Gashpar & Ronto (1980). That paper deals with obtaining X-ray small-angle scattering for a wide range of angles and determining a number of general features and the model of phage T7 based on this curve. The direct method described above was applied to interpret a part of the curve in Fig. 9. The parameters R, ρ_{min}, ρ_{max} and a set of harmonics were chosen using the features specified from the X-ray curve itself and from additional information. The restored electron density distribution in the cross section containing the phage axis of rotational symmetry is shown in Fig. 10. The radial and angular resolutions are about 12 Å and 25° respectively (the center of polar coordinates placed at point 0). The projection of the phage head looks like a smoothed hexagon with each side about 350 Å (suggesting that the head is likely to be icosahedral in shape), the tail being a right circular cylinder with radius 110 Å and height 180 Å. There is a globular protein core in the central part of the head with

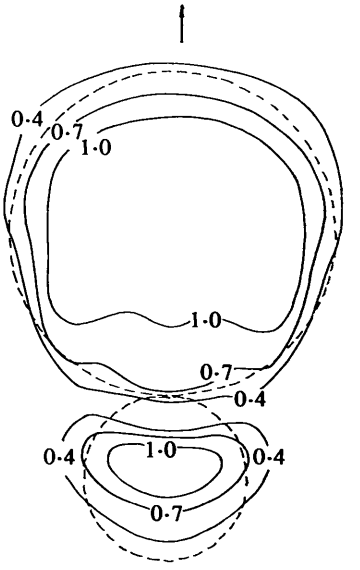

Fig. 8. The reconstruction of the model body consisting of two touching solid spheres. The density $\rho(\mathbf{r}) = 1$, radii of spheres $R_1 = 54{\cdot}5$, $R_2 = 27{\cdot}3$. The cross section containing the rotation axis (specified by an arrow) is shown. Dashed line: the cross section of the spheres. Solid lines: isolines of restored structure (eighth iteration); the restrictions are $\rho_{min} = -0{\cdot}2$, $\rho_{max} = 1{\cdot}5$; numbers of harmonics $l = 0, 1, 2, 3$; $R_l = 5{\cdot}5 \times 10^{-3}$; $R = 100$, $s_{max} = 0{\cdot}5$.

diameter 240 Å. This neatly agrees with the results of Agamalian *et al.* (1982). One observes also a cylindrical region of higher density with diameter 80 Å near the tail, revealing a high concentration of slightly hydrated DNA. On the whole, the phage DNA is hydrated more strongly than the protein, as expected (see Rolbin, Svergun, Feigin, Gashpar & Ronto, 1980). The density levels corresponding to the density of a somewhat higher level than that of the protein appear to be the traces of the regular arrangement of DNA within the phage head. The fact that they are concentric arcs is in favor of the assumption that DNA packs into concentric spherical layers (see Earnshaw & Harrisson, 1977). The scattering curve of the restored structure is shown in Fig. 9 and coincides accurately with the experimental one up to the s values corresponding to radial resolution.

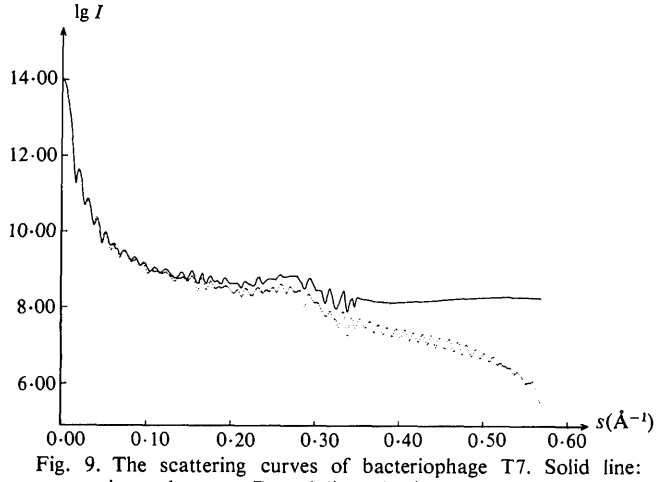

Fig. 9. The scattering curves of bacteriophage T7. Solid line: experimental curve. Dotted line: the intensity of the restored structure.

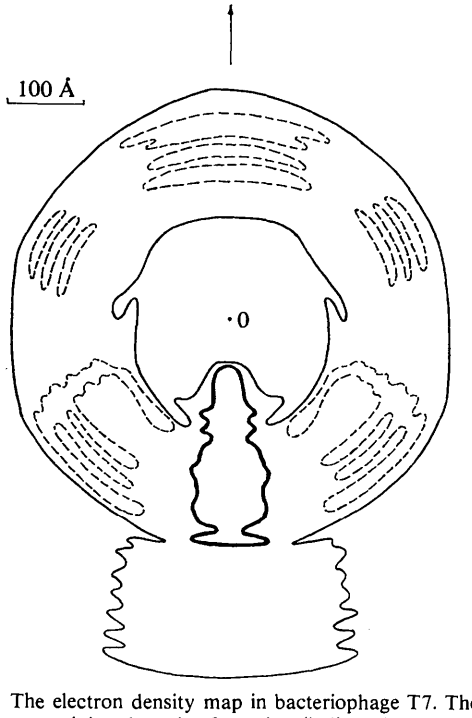

Fig. 10. The electron density map in bacteriophage T7. The cross section containing the axis of rotation (indicated by an arrow) is shown. Solid line: level 0·38 Å^{-3} (hydrated protein); dashed line: 0·42 Å^{-3} (strongly hydrated DNA); thick line: 0·52 Å^{-3} (slightly hydrated DNA). The result of the ninth iteration is given, $R_I = 2{\cdot}2 \times 10^{-2}$.

Conclusions

The procedure has been developed to achieve the decomposition of small-angle scattering intensity by dilute systems of identical particles into a multipole expansion. The limitation conditions concerned with particle dimensions and density range are sufficient for it to operate.

In the spherically symmetric case the solution is unique (except for a factor ± 1); in the axially symmetric case the number of possible structures equals 2^{M-2}, where M is the number of harmonics approximating the intensity curve ($M = 4$–5 as a rule). In the general case, to restore the structure additional information is required. As to the errors involved in the input parameters (restrictions, set of harmonics, intensity curve), the method proves to be stable enough.

The application of the proposed method to the small-angle X-ray scattering curve of bacteriophage T7 permitted for the first time the structure of a biological macromolecule to be obtained based on small-angle scattering data. All T7 structural features specified are in good agreement with the data provided by other methods.

The authors are greatly indebted to Acad. B. K. Vainshtein for his constant interest and helpful comments in the course of our study.

APPENDIX *A*

The convergence of the iterative procedure in reciprocal space

Let us consider the difference

$$I(s) - I^{(k)}(s) = 2\pi^2 \sum_{l=0}^{L} [A_l^2(s) - A_l^{(k)2}(s)]$$

$$\simeq 2\pi^2 \sum_{l=0}^{L} \Delta_l(s)\, A_l^{(k)}(s) \times \{1 + [I(s)/I^{(k)}(s)]^{1/2}\}, \quad (12)$$

where $\Delta_l(s) = A_l(s) - A_l^{(k)}(s)$. The approximate equation was obtained assuming $\Delta_l(s) \ll A_l(s)$. It seems natural to suppose that the corrections to the partial amplitudes are proportional to their values

$$\Delta_l(s)/A_l^{(k)}(s) = \Delta_j(s)/A_j^{(k)}(s) \quad (13)$$

(for $0 \le i \le L$, $0 \le j \le L$). Solving the system (12) and (13), one gets

$$\Delta_l(s) = A_l^{(k)}(s)\,\{[I(s)/I^{(k)}(s)]^{1/2} - 1\}. \qquad (14)$$

Had corrections to radial functions been calculated from $\Delta_l(s)$, they would have ensured the coincidence of $I^{(k+1)}(s)$ and $I(s)$. Now let us note that the addition of $A^{(k)}(s)$ to both parts of (14) results in (8). The multiplication of the corrections by $\prod (r - R)$ according to (9) distorts the equivalence of $I^{(k+1)}(s)$ with $I(s)$, and yet the trend of convergence remains.

APPENDIX *B*
The reduction of the termination effects

In the case of finite range intensity specified, the transformation (5) appears as

$$\tilde{\rho}_{lm}(r) = (-i)^l (2/\pi)^{1/2} \int_0^{s_{\max}} s^2 A_{lm}(s)\, j_l(sr)\, \mathrm{d}s. \qquad (15)$$

The function $\tilde{\rho}_{lm}(r)$ contains the 'termination waves' similar to the Gibbs effect in the Fourier transform. It may be shown that the operator

$$\Phi_l[\tilde{\rho}_{lm}(r)] = \frac{l+2}{(r+t)^{l+2} - (r-t)^{l+2}} \int_{r-t}^{r+t} \xi^{l+1}\, \tilde{\rho}_{lm}(\xi)\, \mathrm{d}\xi, \qquad (16)$$

where $t = \pi/s_{\max}$, is equivalent to the application of the σ multiplier of Lanczoc (Hamming, 1962) for the sine Fourier transform. This operator reduces the termination waves, preserving the slowly changing [with respect to $\sin(s_{\max} r)$] function $\rho_{lm}(r)$. In the particular case $l = 0$ (most widely used in small-angle scattering) (Rolbin, Svergun, Feigin & Schedrin, 1980), the efficiency of this 'generalized Steklov filter' was demonstrated by comparing the latter with the 'temperature multiplier' method (Waser & Schomaker, 1953).

APPENDIX *C*
The calculation of the corrections to the radial functions using density restrictions

It is necessary to find $L + 1$ functions $\Delta\rho_l(r)$ to meet the requirements

$$\rho_{\min} - \rho^{(k)}(\mathbf{r}) \le \Delta\rho(\mathbf{r}) \le \rho_{\max} - \rho^{(k)}(\mathbf{r}) \qquad (17)$$

and

$$\min\left(\int_0^{\infty} s^4 \{I(s) - 2\pi^2 \sum_{l=0}^{L} [A_l^{(k)}(s) - A_l(s)]^2\}^2\, \mathrm{d}s \right), \qquad (18)$$

where

$$\Delta\rho(\mathbf{r}) = \sum_{l=0}^{L} \Delta\rho_l(r)\, Y_{l0}(\theta), \quad 0 \le r \le R, \quad 0 \le \theta \le \pi,$$

and $\Delta A_l(s)$ are connected with $\Delta\rho_l(r)$ by transformations (4).

To perform the Hankel transforms involved with corrections it is convenient to use Laguerre polynomials $L_n^{(\alpha)}(x)$ (see *Handbook of Mathematical Functions*, 1964). Since

$$(2/\pi)^{1/2} \int_0^{\infty} r^l \exp(-r^2/2)\, L_n^{(l+1/2)}(r^2)\, j_l(sr)\, r^2\, \mathrm{d}r = (-1)^n s^l \exp(-s^2/2)\, L_n^{(l+1/2)}(s^2) \qquad (19)$$

(see Stuhrmann, 1970), then, supposing that

$$\Delta\rho_l(r) = r^l \exp(-r^2/2) \sum_{n=0}^{K} c_{ln} L_n^{(l+1/2)}(r^2), \qquad (20)$$

one obtains

$$\Delta A_l(s) = s^l \exp(-s^2/2) \sum_{n=0}^{K} (-1)^n c_{ln} L_n^{(l+1/2)}(s^2). \qquad (21)$$

Here K is the maximal order of Laguerre polynomials, and c_{ln} are constants to be determined.

Inserting (20) and (21) into (17) and (18) one arrives at the task of non-linear programming with respect to coefficients c_{ln} (Karmanov, 1975). Assuming the corrections to be small enough, the $\Delta A_l(s)$ squared terms can be neglected in (18), hence leading to the task

$$\min \sum_{\nu=1}^{\beta} b_\nu x_\nu \qquad (22)$$

$$\sum_{\nu=1}^{\beta} a_{\mu\nu} x_\nu \ge d_\mu, \quad 1 \le \mu \le \alpha, \qquad (23)$$

where

$$b = b_{ln} = (-1)^n \int_0^{\infty} s^4 A_l^{(k)}(s)\,[I^{(k)}(s) - I(s)] \exp(-s^2/2) \times s^l L_n^{(l+1/2)}(s^2)\, \mathrm{d}s,$$

$x_\nu = c_{ln}$, $\beta = (L + 1)(K + 1)$, $l = \{(\nu - 1)/K\}$, $n = \nu - (K + 1)\, l - 1$, α is the number of restrictions, $\alpha > \beta$, r_μ, θ_μ are a grid of restrictions,

$$a_{\mu\nu} = r^l \exp(-r_\mu^2/2)\, L_n^{(l+1/2)}(r^2)\, (-1)^\mu\, Y_{l0}(\theta_\mu),$$

$$d_\mu = \{[1 - (-1)^\mu]/2\}\,[\rho^{(k)}(r_\mu, \theta_\mu) - \rho_{\max}] + \{[1 + (-1)^\mu]/2\}\,[\rho_{\min} - \rho^{(k)}(r_\mu, \theta_\mu)].$$

Conditions (22) and (23) represent the standard form of the problem of linear programming (Dantzig, 1963); its vector of solution provides us with coefficients c_{ln} determining, according to (20), the required corrections. To solve the task a modified simplex method (Dantzig, 1963) was used. As to the validity of the linearization of (18), one may judge it by the alterations in R_I factor following the above mentioned performance.

References

AGAMALIAN, M. M., DRABKIN, G. M., DOVJIKOV, A. A., KRIVSHICH, T. I., LVOV, YU. M., FEIGIN, L. A., RONTO, G. & GASHPAR, SH. (1982). *Kristallografiya*, **27**, 92–96.

DANTZIG, G. B. (1963). *Linear Programming and Extensions*. New Jersey: Princeton Univ. Press.

EARNSHAW, W. C. & HARRISSON, S. C. (1977). *Nature (London)*, **258**, 598–602.

GLATTER, O. (1979). *J. Appl. Cryst.* **12**, 166–175.

GLATTER, O. (1981). *J. Appl. Cryst.* **14**, 101–108.

GUINIER, A. & FOURNET, G. (1955). *Small-Angle Scattering of X-rays*. New York: Wiley.

HAMMING, R. W. (1962). *Numerical Methods for Scientists and Engineers*. New York: McGraw-Hill.

Handbook of Mathematical Functions (1964). Edited by M. ABRAMOVITZ & I. A. STEGUN. Washington: Government Printing Office.

KARMANOV, V. G. (1975). *Matematicheskoe Programmirovanie*. Moscow: Nauka.

MARGUERIE, G. & STUHRMANN, H. B. (1976). *J. Mol. Biol.* **102**, 143–156.

ROLBIN, YU. A., SVERGUN, D. I., FEIGIN, L. A., GASHPAR, SH. & RONTO, G. (1980). *Dokl. Acad. Nauk SSSR*, **255**, 1497–1500.

ROLBIN, YU. A., SVERGUN, D. I., FEIGIN, L. A. & SCHEDRIN, B. M. (1980). *Kristallografiya*, **25**, 1125–1128.

SNEDDON, I. (1951). *Fourier Transforms*. New York: McGraw-Hill.

STUHRMANN, H. B. (1970). *Acta Cryst.* A**26**, 297–306.

STUHRMANN, H. B. & FUESS, H. (1976). *Acta Cryst.* A**32**, 67–74.

STUHRMANN, H. B. & KIRSTE, R. G. (1965). *Z. Phys. Chem. (Frankfurt am Main)*, **46**, 247–250.

SVERGUN, D. I., FEIGIN, L. A. & SCHEDRIN, B. M. (1982). *Kristallografiya*, **27**. In the press.

WASER, J. & SCHOMAKER, V. (1953). *Rev. Mod. Phys.* **26**, 671–690.

Acta Cryst. (1982). A**38**, 835–840

A Theory for the Evaluation of Small-Angle Scattering Diagrams of Quasi Radially Symmetric Particles Considering Polydispersity and Deviations from Radial Symmetry

BY M. BAUMSTARK, W. WELTE AND W. KREUTZ

Institut für Biophysik und Strahlenbiologie der Universität Freiburg im Breisgau, Albertstrasse 23, *D*-7800 *Freiburg, Federal Republic of Germany*

(*Received* 26 *April* 1982; *accepted* 21 *June* 1982)

Abstract

A general theory has been developed describing the scattering intensity of a polydisperse dilute ensemble of particles. These particles are assumed to be mainly radially symmetric. Deviations from radial symmetry are treated quantitatively using an expansion of the electron density in terms of multipole components. The particle radii are assumed to have a Gaussian-like distribution. The electron density of the particle core is allowed to be different from that of the solvent. As a practical application of this theory a Fortran 77 program was written which determines the radial electron density profile, the standard deviation of the radii, and additional parameters describing the deviations from spherical symmetry directly from the measured intensity.

I. Introduction

Theoretical expressions for the small-angle scattering of polydisperse membrane vesicles were given by Weick, Hosemann, Pape & Menke (1974) and Moody (1975). Moody's theory is exact in the case of polydisperse ensembles with electron density of the particle core being equal to that of the solvent. The theory given by Weick *et al.* is an approximation of that given by Moody. Only Weick *et al.* give a concrete representation of the model electron density and the statistical function describing radius variations. This concrete representation is, however, essential for a practical application of the theory to evaluate scattering diagrams. Both theories do not include deviations from spherical symmetry.

In this paper a general theory is developed taking into account polydispersity and electron density difference between particle core and solvent, as well as non-radially-symmetric parts of the particle structure. The contributions of the non-radially-symmetric parts are quantitatively estimated, using an expansion of the electron density in terms of spherical harmonics, which was introduced by Stuhrmann (1970) to describe arbitrary one-particle scattering functions. In contrast to Stuhrmann's theory it is necessary for our theory, dealing with ensembles of particles, to consider effects of polydispersity on the multipole components.

0567-7394/82/060835-06$01.00